Torque Ripple Minimization in Synchronous Reluctance Motor Using a Sinusoidal Rotor Lamination Shape

M. Muteba, *Member*, *IEEE*, B. Twala, *Senior Member*, *IEEE* and D. V. Nicolae, Member, *IEEE*

***Abstract* – A Synchronous Reluctance Motor (SynRM), which has sinusoidal rotor lamination shape in the axial direction, is proposed. The sinusoidal lamination shape is utilized to vary the magnetic flux in the *q*-axis direction. Therefore, cancelling some torque harmonics produced by slotting effects. The stator geometry of a 1.5 kW, conventional three-phase squirrel cage induction motor, with distributed double layer winding, chorded by one slot, is used for both basic and proposed models. Due to the axial geometry design of sinusoidal lamination shape for the proposed model, 3-D Finite Element Method (FEM) is used for dynamic analysis. From the FEM results, it evidenced that with current vector angle of 45^{o}electric, the proposed model reduced the torque ripple content by more than 60 % and still maintained the average torque.**

***Keywords*—**Finite Element Method (FEM), Sinusoidal rotor Lamination Shape, Synchronous reluctance motor, Torque Ripple Minimization.

I. Introduction

The SynRMs have high torque density, fault-tolerant capability, high efficiency, low rotor inertia and simple controllability in comparison with induction machines [1], [3]. Despite several advantages, one of common problems of SynRMs is the high contents of torque ripples [2], [4]. This is due to the interaction between spatial harmonics of the electrical loading and the rotor anisotropy which causes a high torque ripple that is intolerable in the most of applications [5]-[7].

Several efforts have been made to mitigate torque ripples in SynRMs. It is reported in [7] that the skewing of the rotor by a stator slot pitch reduces the slot torque harmonic, but it also drops the average torque.

In [8] it has been shown that a reduction of torque ripple can be achieved by means of a suitable choice of number of flux-barriers with respect to the number of stator slots per pole pair. The flux-barrier ends are uniformly distributed along the airgap (similarly to the stator slot distribution). Torque ripple reduction for SynRMs using asymmetric flux barrier has been reported in [2]. The method consists of shifting the relative position between the edge of each flux barrier and stator teeth by a certain angle. In [9], asymmetric flux barrier angles and a flipped rotor structure have been presented as an approach of torque ripple reduction without losing the average torque. Elsewhere a novelty strategy to compensate the torque harmonics of the SynRMs has been presented in [4] and [5]. The method is achieved by forming the rotor with lamination of two different kinds called "Romeo (R-type) and Juliet (J-type)". The "R-type and J-type" rotors are formed by lamination of two different kinds.

Furthermore, an alternative design was presented in which a single lamination is used with flux barriers that exhibit a different geometry under various poles, aiming indeed to cancel the torque harmonic of one order and to compensate those of other orders [5]. This configuration can be looked upon as an evolution of the "R-type and J-type" configurations [5], and then called the "Machaon" configuration [4].

From the above, it is noticed that previous work that intended to reduce the torque ripple contents of transverse-laminated synchronous reluctance machines (TLSynRMs), directed their focus mostly on suitable choice of number of flux-barriers respect to the number of stator slots per pole per phase [8], [13], the optimization and asymmetry of the flux-barriers geometry, etc., [2], [4], [5], [6], [9].

In [12], the material-efficient Permanent Magnet Synchronous motor with sinusoidal magnet shape was proposed and analyzed. The magnet shape provides a sinusoidal magnetic flux in order to obtain better sinusoidal electromotive force, less cogging torque and smooth electromagnetic torque. The analysis was performed on fraction of Horse power (Hp) permanent magnet surface-mounted motors used in automotive actuators. For a total rotor volume of 86.6 cm^3, the magnet volume of 18.2 cm^3 for the proposed synchronous permanent motor with sinusoidal permanent magnet shape was obtained.

Though, both Finite Element Analysis (FEA) and practical results presented in [12] are satisfactory, the use of the proposed motor is limited to a fraction of Hp application. For medium and high power motors for use in traction, electric vehicles and hybrid electric vehicles, where less torque ripple and high torque density are required, the magnet volume will be intolerably high.

In this paper, A TLSynRM having sinusoidal lamination rotor shape in the axial direction, without changing the flux barrier geometry, is proposed. There is no magnet on the rotor. The magnetic flux is obtained due to excitation of a symmetric distributed three-phase stator winding.

M. Muteba is with the University of Johannesburg, Department of Electrical Engineering Technology, PO Box 17011 Doornfontein, 2023, Johannesburg, South Africa (e-mail: mmuteba@uj.ac.za).
B. Twala is with University of Johannesburg, Department of Electrical and Electronic Engineering Science, PO Box 524 Auckland Park, 2006, Johannesburg (E-mail: btwala@uj.ac.za).
D.V. Nicolae is with University of Johannesburg, Department of Electrical Engineering Technology, PO Box 17011 Doornfontein, 2023, Johannesburg (E-mail: danaurel@yebo.co.za).

978-1-5090-2537-4/16/$31.00 ©2016 IEEE

II. Motor Basic Model

Fig.1 shows the cross-section of the basic model with cut-off along the *q*-axis near the airgap.

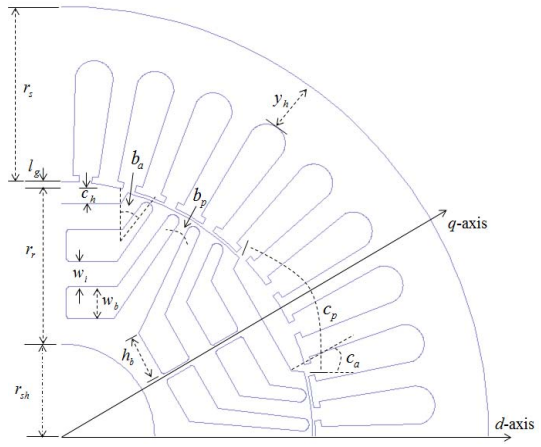

Fig.1. Cross-section of the basic model with cut-off on the *q-axis*

Table I gives the design specifications of the basic model, while Fig.2 illustrates in 3-D view the stator and rotor cores for the basic model.

TABLE I
SPECIFICATIONS OF THE BASIC MODEL

Description	Value	Unit
Airgap length_l_g	0.45	mm
Barrier angle_ b_a	6.69	Degree_*mech*
Barrier pitch_ b_p	5.00	Degree_*mech*
Barrier width_w_b	5.00	mm
Cut-off angle_c_a	2.00	Degree_*mech*
Cut-off height_c_h	3.05	mm
Cut-off pitch_c_p	30.00	Degree_*mech*
Horizontal barrier length_h_b	7.50	mm
Iron width_w_b	4.00	mm
Lamination axial length_l_s	112.00	mm
Number of barriers per pole	2	-
Number of pole pairs	3	-
Number of stator slots	36	-
Ratio insulation to iron on *q-axis*	1.08	-
Rotor radius_r_r	25.05	mm
Stator outer diameter_D_o	135.00	mm
Stator radius_r_s	27.50	mm
Shaft radius_r_{sh}	14.50	mm
Yoke height_y_h	12.50	mm

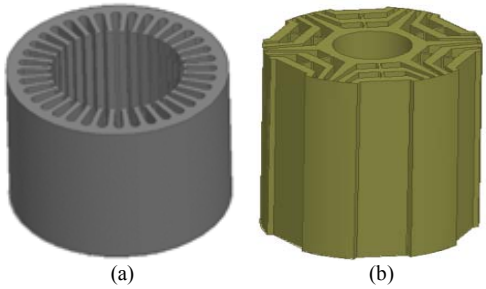

(a) (b)

Fig.2. Configuration of the basic model, (a) Stator core and (b) rotor core

III. Proposed Model With Axially Sinusoidal Lamination Shape

A. Design Concept

The proposed model consists of different laminations having the same flux barrier geometric parameters and different cut-off pitch angles near the airgap along the *q*-axis direction. The cut-off height "c_h" is kept constant. The cut-off pitch angle "C_p" and the cut-off angle "C_a" are varied. C_p is varied by a fifth of the stator slot pitch while the cut-off angle is varied by a relatively very small value. The variation of cut-off pitch and cut-off angle of the proposed model is expressed as

$$\Delta c_p = 3\alpha_s \le c_{p_n} \ge \frac{\alpha_s}{5} \quad (1)$$

$$\Delta c_a = \frac{\alpha_s}{5} \le c_{a_n} \ge \frac{\alpha_s}{10} \quad (2)$$

Where α_s is the stator slot pitch and c_{pn} is the cut-off pitch in mechanical degree for lamination "n". For n_1, the cut-off pitch c_{p1} is 30^0mechanical. Fig. 3 shows the proposed model with cut-off pitch angle that varies in the *q*-axis direction.

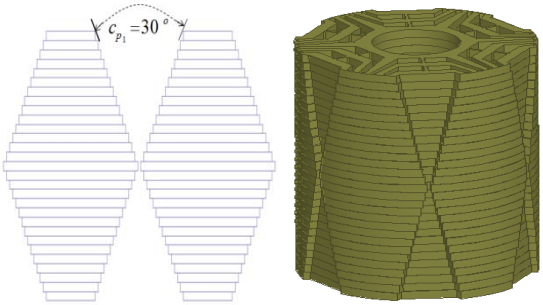

(a) (b)

Fig.3. Proposed model (a) cross-section of axially sinusoidal lamination shape, (b) 3D view of the rotor core.

It should be noted that the optimization of the flux barrier geometry, to cancel some torque harmonics in both basic and proposed models was not performed. There is no skew in the design. A saliency ratio of 10.7 was achieved. Neglecting saturation, field weakening ratio of 5.4 and maximum power factor of 0.83 were obtained.

B. Flux Density Distribution

Fig.4 shows the magnetic flux density distribution, when the *d*-axis current i_d = 6.48 A and *q*-axis current i_q= 6.48 A are applied. It is observed from Fig.4 that, there is a uniform distribution of flux density on the rotor back iron, in the direction of the *q*-axis of the basic model. The magnitude of the flux density is high on the centre line along the axial length, This is due by the presence of radial ribs in the design to connect the rotor segments to each other and also to provide additional mechanical strengh [8].

Therefore, in the basic model, the flux density distribution is not seriously affected by the *q*-axis current. The evidence is different for the proposed model. In the

axis direction. The flux density distribution varies with the lamination shape along the axial length. It is clear that the *q*-axis current affects the flux density distribution in the proposed model.

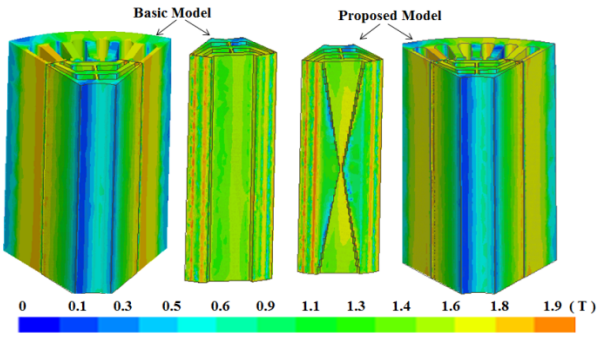

Fig.4. Comparison of flux density distribution of 3D FEA, only a pole is shown.

C. *Flux linkages in rotating reference Frame*

In the proposed model, the cut-off pitch angle is varied along the *q*-axis, therefore changing quantities in the rotating reference frame. The stator flux linkages λ_a, λ_b and λ_c can be directly obtained from FEM. These stator flux linkages are converted into the rotating reference frame. The rotor quantities λ_d, λ_q and λ_o are given by

$$\lambda_d = \frac{2}{3}\left[\lambda_a \cos\theta + \lambda_b \cos\left(\theta - 120^o\right) + \lambda_c \cos\left(\theta + 120^o\right)\right] \quad (3)$$

$$\lambda_q = \frac{2}{3}\left[\lambda_a \sin\theta + \lambda_b \sin\left(\theta - 120^o\right) + \lambda_c \sin\left(\theta + 120^o\right)\right] \quad (4)$$

$$\lambda_o = \frac{1}{3}\left(\lambda_a + \lambda_b + \lambda_c\right) \quad (5)$$

Where θ is the sum of rotational speed ωt and current space phasor (vector) angle ϑ. The stator current is assumed to be sinusoidal, the zero sequence component of the current becomes zero and can be neglected. The current vector angle can be calculated accordingly using

$$\vartheta = \angle I_S = \tan^{-1}\left(\frac{i_q}{i_d}\right) \quad (6)$$

Where I_S is the stator current space phasor, i_d and i_q are the *d*- and *q*-axis currents. Even though the flux linkages have harmonic contents, it is of such nature that the zero sequence flux linkage component λ_o can be neglected and the sum of the linkages λ_d, λ_q, λ_o is approxiatly zero [11].

The flux linkages λ_d and λ_q as function of rotor position are shown in Fig.5, (a) and (b) respectively. The Finite Element Analysis (FEA) was performed at ϑ = 45°electric, i_q= 6.48 A and i_d = 6.48 A. As mentionend in pior section that the three-phase windings are made of distributed double layer chorded coils to produce a sinusoidal inductance-position curve. Therefore, all the flux linkage waveforms are nearly an exact sinusoidal due to the sinusoidal excitation current.

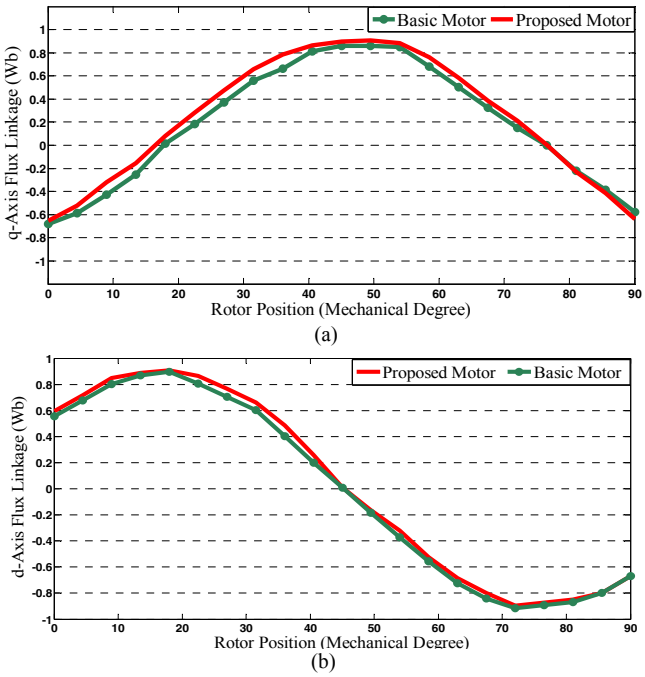

Fig.5. Comparison of Flux Linkages. (a) *q*-axis flux linkage, (b) d-axis flux linkage

VI. Torque And Torque Ripple Analysis

A. *Relationship between torque ripple and variation of d-q axis inductance*

The developed torque for the smooth airgap SynRM is given as [7]:

$$T = \frac{3}{2}\frac{p}{2}\left(L_d - L_q\right) i_d\, i_q = \frac{3}{2}\frac{p}{2}\left(L_d - L_q\right) I_S^2 \sin\left(\vartheta\right) \quad (7)$$

Where p is number of poles, and L_d and L_q are the *d*- and *q*-axis inductances. Analytical torque estimation of SynRMs is well treated in [10] and [11]. If the first harmonic of torque ripples due to the stator slotting is considered the flux linkages and inductances can be expressed as [10]:

$$\begin{bmatrix}\lambda_d \\ \lambda_q\end{bmatrix} = \begin{bmatrix}L_d(\theta) & L_{dq}(\theta \\ L_{dq}(\theta) & L_q(\theta)\end{bmatrix}\begin{bmatrix}i_d \\ i_q\end{bmatrix} \quad (8)$$

$$\frac{\partial \lambda_d}{\partial i_q} = \frac{\partial \lambda_q}{\partial i_d} \quad (9)$$

$$L_d(\theta) \cong L_{do} + \Delta L_d \cos(3pq\,\theta) \quad (10)$$

$$L_q(\theta) \cong L_{qo} - \Delta L_q \cos(3pq\,\theta) \quad (11)$$

$$L_{dq}(\theta) \cong -\Delta L_{dq} \sin(3pq\,\theta) \quad (12)$$

Where q is the number of slots per pole per phase, ΔL_d and ΔL_d being the variation of the *d*- and *q*-axis synchronous inductances, and ΔL_{dq} is the variation of *d*-*q* inductances.

Due to the inductances dependency to rotor angle, a second term which depends of the variation in the *d*- and *q*-

axis flux linkages with each rotor position should be added to (7). The torque equation of the SynRM is expressed as

$$T(\theta) = \frac{3}{2} p\left(i_q \lambda_d - i_d \lambda_q + \frac{1}{2}\left(i_q \frac{\partial \lambda_q}{\partial \theta} + i_d \frac{\partial \lambda_d}{\partial \theta} \right) \right) \quad (13)$$

The average of the second term is zero, but this term dominates when it comes to torque ripple. By introducing inductances dependency to rotor position in the above equation and with stator slot not skewed, the torque is given by

$$T(\theta) = \frac{3}{2}\frac{p}{2}[(L_{do} - L_{qo}) i_d i_q + (\Delta L_d + \Delta L_q) i_d i_q \cos(3pq\theta) - \Delta L_{dq}(i_d^2 - i_q^2)\sin(3pq\theta)] \quad (14)$$

The torque ripple has two components; the first one is proportional to average torque, and the second one is responsible for no-load condition ripple. In the first component of the torque ripple, ΔL_d *is* caused by the oscillation of the Carter's factor, while ΔL_q is mainly related to oscillation of the circulating flux component along the *q*-axis [10].

The proposed model in this paper consists of different laminations having different cut-off pitch angles near the airgap along the *q*-axis, thus forming a sinusoidal shape along the axial length of the rotor. The total axial length of the rotor lamination is equal to

$$Z = 2(\xi_1 + \xi_2 + \xi_3 \ldots + \xi_n) + \upsilon + k_i \quad (15)$$

Where k_i being the total thickness of steel lamination insulation coating, υ is the axial length of the middle lamination shape and ξ *is* the axial length of each individual lamination shape in one half period of the sinusoidal structure.

The torque harmonic produced by ΔL_d and ΔL_q along the positive half period will be the same in magnitude with the harmonic torque produced in the negative half period. The middle lamination structure is having zero cut-off angle, and a minimum cut-off pitch of $\alpha_s/2$. The cut-off opening is equal to the stator slot opening of $b_o = 2$ mm.

The effect of ΔL_d and ΔL_q on the middle lamination will be negligible; the effect on other laminations that form the sinusoidal shape will be cancelled due to the opposite periodicity of the rotor structure. Neglecting the first component of torque ripple as expressed earlier in "(14)", the torque equation can then be written as

$$T(\theta) = \frac{3}{2}\frac{p}{2}[(L_{do} - L_{qo}) i_d i_q - \Delta L_{dq}(i_d^2 - i_q^2)\sin(3pq\theta] \quad (16)$$

The only term that will be highly responsible for torque ripple production is ΔL_{dq}. For the proposed model, the cut-off pitch is varied, thus reducing the insulation on the *q*-axis and increasing the iron on the *d*-axis in the first half period. The action is reversed in the second half period, where the iron on the *d*-axis is reduced and insulation increased on *q*-axis. The ΔL_{dq} is therefore varied, and this variation contributes to the cancellation of some torque harmonics when the rotor sweeps through certain angular positions.

B. Results and Analysis

The torque profiles as function of position are shown in Fig. 6 to Fig. 9. The FEA were carried out at constant speed of 1000-rpm and constant frequency of 50-Hz. Both basic and proposed models have three-phase double layer lap windings chorded by one slot. The windings are excited by 3-phase sinusoidal currents. The SynRMs were started at initial rotor position of 17.5°mechanical, such that phase *A* is opposite to the *d*-axis. The machines were run at different current space phasor angles ϑ.

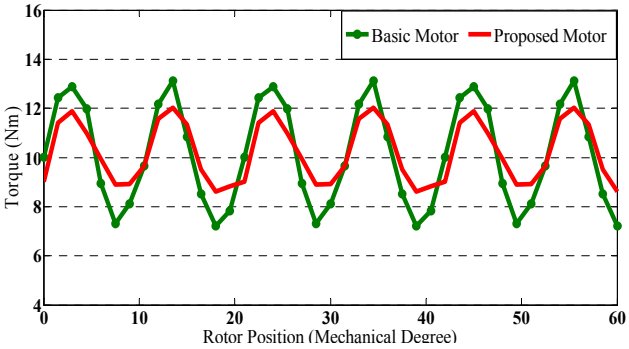

Fig.6. Instantaneous torque as function of rotor position at ϑ=15°, $i_d = 8.85\ A$ & $i_q = 2.37\ A$

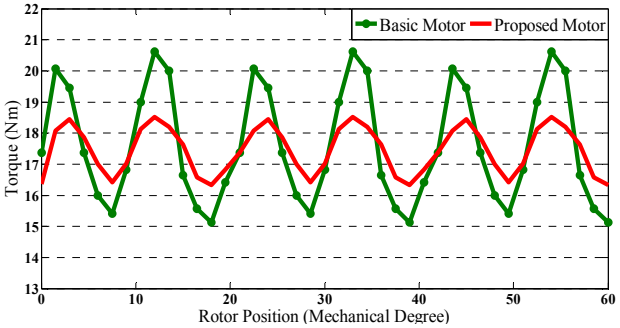

Fig.7. Instantaneous torque as function of rotor position at ϑ=30°, $i_d = 7.93\ A$ & $i_q = 5.58\ A$

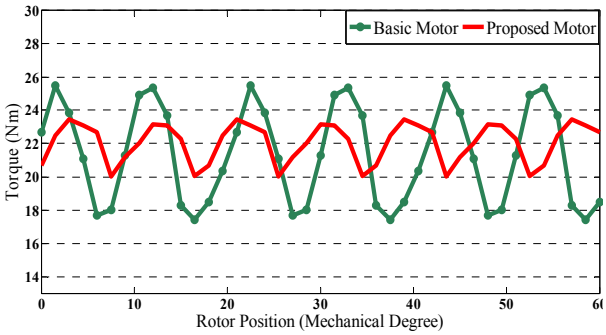

Fig.8. Instantaneous torque as function of rotor position at ϑ=45°, $i_d = i_q = 6.48\ A$

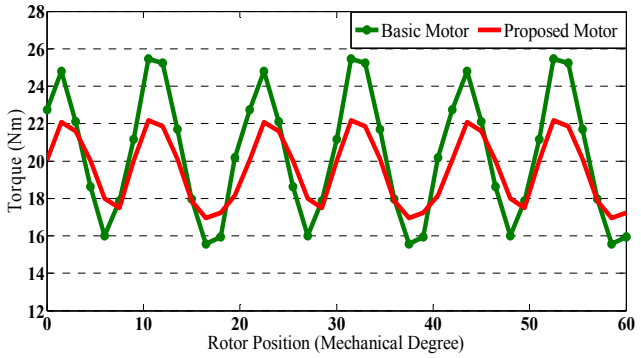

Fig.9. instantaneous torque as function of rotor position at ϑ=60°, $i_d = 4.58\,A$ & $i_q = 7.93\,A$

Table II reports the computed average and torque ripple for different current vector angles of the basic and proposed models. It is clear that the proposed motor has the edge to reduce the torque ripple by ± 60 % for both current vector angles of 30° and 45°electric, and still maintain the average torque. It is also noted that high average torque is achieved with current vector angle of 45°electric.

TABLE II
TORQUE COMPARISON AT DIFFERENT CURRENT VECTOR ANGLES

Current angle ϑ (electrical .degree)	Basic Motor		Proposed Motor	
	$T_{av}(Nm)$	$\Delta T/T_{av}$ (%)	$T_{av}(Nm)$	$\Delta T/T_{av}$ (%)
15	10.07	58.79	10.18	33.58
30	17.56	31.25	17.38	12.58
45	21.32	37.94	22.00	15.50
60	20.38	47.57	19.53	26.73

Table III shows the resulting torque harmonics corresponding to the torque behavior in Fig.6 to Fig.9. The FEA torque harmonics of the Basic Motor (BM) are compared with the torque harmonics of the Proposed Motor (PM).

TABLE III
TORQUE HARMONIC COMPARISON AT DIFFERENT CURRENT ANGLES

Current angle	$\vartheta = 15°$		$\vartheta = 30°$		$\vartheta = 45°$		$\vartheta = 60°$	
Harmonic Order	BM (%)	PM (%)	BM (%)	PM (%)	BM (%)	PM (%)	BM (%)	PM (%)
6	2.18	1.46	3.34	2.01	5.00	4.37	6.57	3.98
12	31.20	19.58	23.19	7.23	22.28	6.02	24.87	16.34
18	2.05	1.27	1.96	0.50	1.58	1.12	1.81	1.13
24	0.71	0.94	0.56	1.24	0.64	0.79	1.39	0.89
30	1.93	1.35	1.70	1.81	1.67	1.55	1.01	1.27
36	1.2	1.06	1.16	0.92	0.79	0.62	1.90	1.11

From Table III, It is interesting to observe that the highest torque harmonics are the first and second slot harmonics, which are the 6th and 12th orders. The latter is the most predominant which contributes to high torque ripple contents. In addition, Table III evidences that the proposed model reduces tremendously the 12th torque harmonics by ±73 % when the current vector angle is 45°electric. At current vector angle of 30°electric, the magnitude of the 12th harmonic order is reduced by ± 69 %.

V. CONCLUSION

A Synchronous Reluctance Motor with sinusoidal rotor lamination shape in the axial direction was proposed. Design approach of the proposed motor was described and, the objective to reduce torque ripple while maintaining high average torque was achieved. A torque ripple factor of 12.58% with current space vector angle of 30°electric, was obtained without optimizing the geometric quantities of flux barriers. The proposed model cancelled some torque harmonics, as consequence the predominant 12th torque harmonic order, due to stator slotting, has been reduced by more than half at current vector angle of 30° and 45°electric. Very low torque ripple factor of less than 10 % can be achieved by combining the proposed model with design optimization of flux barrier geometry. Practical validation of FEA results will be reported in subsequent paper.

VI. REFERENCES

[1] A. Boglietti, A. Cavagnino, M. Pastorelli, and A. Vagati," Experimental comparison of induction and synchronous reluctance motors performance", in *4th IAS annual Meeting. Conference Record of 2005*, vol. 1, Oct 2005, pp. 474-479.

[2] M. Sanada, K. Hiramato, S. Morinoto, and Y. Takeda, "Torque Ripple Improvement for Synchronous Reluctance Motor Using Asymmetric Flux Barrier Arrangement", in *Proc. IEEE Ind. App. Soc. Annual Meeting*, 12-16 Oct. 2003.

[3] A Fratta, A. Vagati, F. Villata, G. Franceschini and C. Petrache, " Design comparison between induction and synchronous reluctance motors", in *Proc. 1994 IEEE International Conference on Electrical Machines*, Sept. 1994, Vol. 3, pp. 329-334.

[4] N. Bianchi, S. Bolognani, D. Bond and M. D. Pre', "Rotor Flux-barrier Design for Torque Ripple Reduction in Synchronous Reluctance Motors", in *Proc. 41th IEEE Conf. On Industry Applications*, 2006, 1193-1200.

[5] N. Bianchi, S. Bolognani, D. Bon, and M. D. Pre', "Rotor Flux-barrier Design for Torque Ripple Reduction in Synchronous Reluctance and PM-Assisted Synchronous Reluctance Motors", *IEEE Trans. on Ind. Appl.*, vol. 45, Issue 3, May-June 2009, pp. 921-928.

[6] N. Bianchi and S. Bolognani, "Reducing Torque Ripple in PM Synchronous Motors by Pole Shifting", in *Proc. 2000 IEEE International Conference on Electrical Machines,* Aug. 2000 Helsinki.

[7] X. L. Bomela and J. Kamper, "Effect of Stator Chording and Rotor Skewing on Performance of Reluctance Synchronous Machines", *IEEE Transaction on Industry Application,* Vol. 38. NO. 1. January/February 2002.

[8] A. Vagati, M. Pastorelli, G. Franceschini and C. Petrache, "Design of low-torque-ripple Synchronous Reluctance Motors", In *Annual Meeting, Proc. IEEE Conf Industry Applications*, LA, 1997, 287-293.

[9] L. Tobias, B. Kerdsup, C. Weiss, R. W. De Doncker. "Torque ripple Reduction in Reluctance Synchronous Machines Using an Asymmetric Rotor Structure", *7th IET International Conference on Power Electronics Machines and Drives* (PEMD2014), Manchester, UK, 8-10 April 2014.

[10] A. Fratta, G. P Troglia, A. Vagati, and F. Villata, "Evaluation of torque ripple in high performance synchronous reluctance motors", *Record of IEEE Industry Application Society Annual Meeting*, I: 163-170, October, Toronto, Canada, 1993

[11] T.A. Lipo, T. J.E Miller, A. Vagati, I. Boldea, L. Malesani and T. Fukao, Synchronous Reluctance Drives. *Tutorial IEEE-IAS Annual Meeting,* October 1994

[12] W. Zhao, T. A Lipo and B. Kwon "Material-efficiency magnet shape for torque pulsation minimization in synchronous permanent motors", *IEEE Trans. On Industrial Electronics*, vol. 61, Issue 10, 2014, pp. 5579-5787.

[13] K. Wang, Z. Q. Zhu, G. Ombach, M. Koch, S. Zhang and J. Xu, " Optimal slot/pole and flux-barrier layer number combinations for synchronous reluctance machines", *2013 8th International*

Conference and Exhibition on Ecological Vehicles and Renewable Energies (EVER 2013), pp 1-8, March 2013, Monte Carlo.

VII. BIOGRAPHIES

Mbika Muteba received the Associate Degree of applied science and technology in electrical engineering from higher institute of technology (ISTC), Katanga, DRC, in 1996. After ten years of industrial experience in electrical machines, machines drives, primary and secondary power distribution networks both in DRC and South Africa, he joined the Tshwane University of Technology, South Africa, in 2006. He received the Bachelor's and Master's degrees of Technology in Electrical Engineering in 2008 and 2013, respectively. He is at his final phase of completing his PhD in Electrical and Electronic Engineering at the University of Johannesburg.

Muteba is imployed on permanent basis as a lecturer in the Department of Electrical and Electronic Engineering Technology at the University of Johannesburg. His research interests are design and control of electrical machines for future Electric and Hybrid Electric Vehicles.

Bhekisipho Twala is a Professor in Artificial Intelligence and Statistical Science and the Director of the newly established Institute for Intelligent Systems at the University of Johannesburg (UJ) in South Africa. Before then, he was Head of the Electrical and Electronic Engineering Science Department at UJ and Principal Research Scientist at the Council of Science and Industrial Research (CSIR) within the Modelling and Digital Science Unit. His research work involved an expanded swath of data, analytics, and optimization approaches that brings a more complete understanding of digital customer experiences. Prof Twala's current work involves promoting and conducting research in artificial intelligence within the electrical and electronic engineering science fields and developing novel and innovative solutions to key research problems in these areas.

He earned his Bachelor's degree in Economics and Statistics from the University of Swaziland in 1993; followed by an MSc in Computational Statistics from Southampton University (UK) in 1995; and then a PhD in Machine Learning and Statistical Science from the Open University (UK) in 2005.

Prof. Twala was a post-doctoral researcher at Brunel University in the UK, mainly focussing on empirical software engineering research and looking at data quality issues in software engineering. His broad research interests include multivariate statistics, classification methods, knowledge discovery and reasoning with uncertainty, sensor data fusion and inference, and the interface between statistics and computing. He has particular interests in applications in finance, medicine, psychology, software engineering and most recently in robotics and has published over 70 scientific papers.

Prof. Twala has a wide ranging work experience to organisations ranging from banks, through universities, to governments. He is currently an associate editor of the Intelligent Data Analysis Journal, Journal of Computers, International Journal of Advanced Information Science and Technology, International Journal of Big Data Intelligence, Journal of Image and Data Fusion, Journal of Information Processing Systems, and a fellow of the Royal Statistical Society. Other professional memberships include the Association of Computing Machinery (ACM); the Chartered Institute of Logistics and Transport (CIT), South Africa and a senior member of the Institute of Electrical and Electronics Engineers (IEEE).

Dan Valentin Nicolae, born in Romania 18/09/1948, has got his first degree Master in (Applied) Electronic Engineering in 1971 from University Polytechnic of Bucharest, Romania. Between 1971 and 1975 he was with Institute for Nuclear Technologies as design engineer, than in 1975 he joined National Institute for Scientific and Technical Creativity – Avionics Branch in Bucharest Romania as principal researcher.

In 1998, D. V. Nicolae joined Tshwane University of Technology as lecturer for heavy current subjects. In 2000 he started his research activity in TUT with a stage in France; with this opportunity he started his PhD which has been finalized in 2004. In 2015 he joined University of Johannesburg. Presently, Prof. DV Nicolae is involved in research in power converters for power systems, electric machines, power systems and renewable energy.